10-1-2018

Folding of Gα Subunits: Implications for Disease States

Matthew Najor
Loyola University Chicago

Brian D. Leverson
Loyola University Chicago

Jesse L. Goossens
Loyola University Chicago

Saad Kothawala
Loyola University Chicago

Kenneth W. Olsen
Loyola University Chicago

See next page for additional authors

Recommended Citation

Najor, Matthew; Leverson, Brian D.; Goossens, Jesse L.; Kothawala, Saad; Olsen, Kenneth W.; and de Freitas, Duarte Mota. Folding of Gα Subunits: Implications for Disease States. ACS Omega, 3, 10: 12320-12329, 2018. Retrieved from Loyola eCommons, Chemistry: Faculty Publications and Other Works, http://dx.doi.org/10.1021/acsomega.8b01174

ACS OMEGA

Article

Cite This: ACS Omega 2018, 3, 12320−12329

http://pubs.acs.org/journal/acsodf

Folding of G_α Subunits: Implications for Disease States

Matthew Najor,[†] Brian D. Leverson,[†] Jesse L. Goossens, Saad Kothawala, Kenneth W. Olsen, and Duarte Mota de Freitas*

Department of Chemistry and Biochemistry, Loyola University Chicago, 1032 West Sheridan Road, Chicago, Illinois 60660, United States

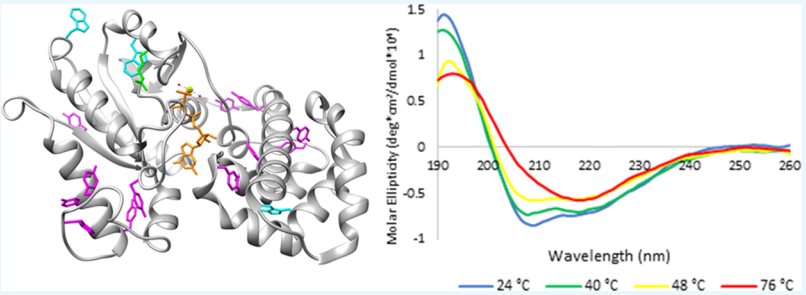

ABSTRACT: G-proteins play a central role in signal transduction by fluctuating between "on" and "off" phases that are determined by a conformational change. cAMP is a secondary messenger whose formation is inhibited or stimulated by activated $G_{i\alpha1}$ or $G_{s\alpha}$ subunit. We used tryptophan fluorescence, UV/vis spectrophotometry, and circular dichroism to probe distinct structural features within active and inactive conformations from wild-type and tryptophan mutants of $G_{i\alpha1}$ and $G_{s\alpha}$. For all proteins studied, we found that the active conformations were more stable than the inactive conformations, and upon refolding from higher temperatures, activated wild-type subunits recovered significantly more native structure. We also observed that the wild-type subunits partially regained the ability to bind nucleotide. The increased compactness observed upon activation was consistent with the calculated decrease in solvent accessible surface area for wild-type $G_{i\alpha1}$. We found that as the temperature increased, G_α subunits, which are known to be rich in α-helices, converted to proteins with increased content of β-sheets and random coil. For active conformations from wild-type and tryptophan mutants of $G_{i\alpha1}$, melting temperatures indicated that denaturation starts around hydrophobic tryptophan microenvironments and then radiates toward tyrosine residues at the surface, followed by alteration of the secondary structure. For $G_{s\alpha}$, however, disruption of secondary structure preceded unfolding around tyrosine residues. In the active conformations, a π-cation interaction between essential arginine and tryptophan residues, which was characterized by a fluorescence-measured red shift and modeled by molecular dynamics, was also shown to be a contributor to the stability of G_α subunits. The folding properties of G_α subunits reported here are discussed in the context of diseases associated to G-proteins.

1. INTRODUCTION

Guanine nucleotide-binding proteins (G-proteins) represent a family of proteins involved in intricate networks of intercellular signaling. Heterotrimeric G-proteins are comprised of α, β, and γ subunits that interact with transmembrane G-protein-coupled receptors (GPCRs). Upon activation of a receptor by an extracellular stimulus, the α-subunit undergoes a conformational change that allows exchange of guanine diphosphate (GDP) for guanine triphosphate (GTP) with concurrent dissociation from the $\beta\gamma$-dimer and GPCR, and a further relay of a signal via an interaction with an intracellular effector. The signal terminates following hydrolysis of the bound GTP, thereby returning the α-subunit back to its inactive state and its reassociation with the $\beta\gamma$ heterodimer and the GPCR.[1−3] Although there are four families of G_α proteins, we limited this study to $G_{i\alpha1}$ and $G_{s\alpha}$, which stimulate or inhibit the production of cAMP by regulating the activity of adenylyl cyclase (AC).

The crystal structures from $G_{i\alpha1}$ in the inactive GDP-bound conformation, as well as from the active states of both $G_{i\alpha1}$ and $G_{s\alpha}$ using GTPγS, a nonhydrolyzable GTP analog, have been solved.[4−6] The crystal structure of $G_{s\alpha}$ complexed with the target AC is also known.[6] G_α is composed of two domains: the α-helical domain and the GTPase domain. The α-helical domain consists of six α-helices that form a lid over the guanine nucleotide-binding site of the GTPase domain. The GTPase domain is composed of six-stranded β-sheets surrounded by five α-helices and in addition to the nucleotide-binding site, the GTPase domain also contains binding sites for the $G_{\beta\gamma}$ dimer and the GPCR. Also, in the GTPase domain are the switch regions known as switches I−III that are located near the nucleotide-binding site. The switch regions undergo a drastic structural change when going from the inactive GDP-bound conformation to the active GTP-bound conformation.[7] In GDP-bound $G_{i\alpha1}$, switch II and switch III are disordered in the X-ray structure, but upon

Received: May 29, 2018
Accepted: September 18, 2018
Published: October 1, 2018

DOI: 10.1021/acsomega.8b01174
ACS Omega 2018, 3, 12320−12329

activation, they become ordered around the γ-phosphate of GTP.[4,5,8]

Protein folding is a complicated and yet a surprisingly efficient event that is critical for protein viability. Protein folding is driven primarily by noncovalent interactions and proceeds through an energy landscape from its unfolded state to its native conformation.[9−12] The free energy of the native state is lower than that of the unfolded protein, which is in equilibrium with molten globules that have a native-like structure. When a protein denatures, it does not go directly to a random coil, but rather to one of these molten globule states, which resembles the native state and may be able to bind a ligand and retain some activity.[13−15] Improper folding of the molten globules can have devastating consequences and is the cause of many diseases.[16]

Hydrophobic interactions contribute the most toward protein stability, but other interactions, such as hydrogen bonding and electrostatic interactions, are important as well.[6] Tryptophan (W) residues are uncommon and play a key role in protein stability via hydrophobic interactions at the core of the protein. $G_{i\alpha1}$ contains three W residues, whereas $G_{s\alpha}$ has four. The W residues in $G_{i\alpha1}$ are W131, W211, and W258 (depicted in cyan in Figure 1), which respectively correspond to W154, W234, and W277 in $G_{s\alpha}$. There is an additional W residue in $G_{s\alpha}$, W281, that has no corresponding equivalent in $G_{i\alpha1}$. Gilman and co-workers reported that intrinsic W fluorescence could be used to investigate conformational changes in G_α proteins that occur during activation because the fluorescence intensity increases when individual W residues move toward a more hydrophobic environment.[17,18] Najor et al. built upon this property to quantify the contribution of each W residue toward the overall fluorescence by using phenylalanine (F) mutants of $G_{i\alpha1}$.[19] We explored this feature to determine the stability at the core of the protein by determining melting temperatures (T_m) from wild-type (WT) and W mutants of $G_{i\alpha1}$ and $G_{s\alpha}$. In addition, a π-cation interaction between W211 and R208 (W234 and R231 in $G_{s\alpha}$) is present in the active conformations of WT G_α proteins, which can be detected by red shifts in their fluorescence emission spectra. Disrupting the π-cation interaction may also have consequences for stability.[20]

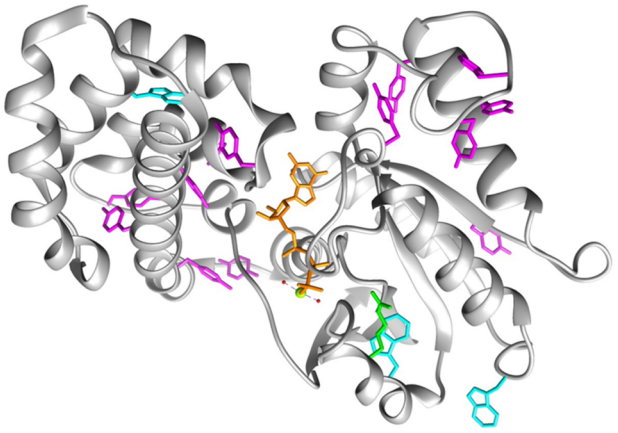

Figure 1. WT $G_{i\alpha1}$·GTPγS displaying its 3 tryptophan residues (cyan), 13 tyrosine residues (purple), R208 (green), GTPγS-bound nucleotide (orange), and Mg^{2+} (green sphere).

Both $G_{i\alpha1}$ and $G_{s\alpha}$ have an abundance of tyrosine (Y) residues (13 for $G_{i\alpha1}$ and 14 in $G_{s\alpha}$) (Figure 1) from which we can take advantage of the UV absorbance to determine the T_m values at the surface of the protein for WT and W mutants. Although Y as well as W residues absorb light at 280 nm, in both G_α proteins Y residues far outnumber W amino acids resulting in absorbance changes that are dependent on Y and W residues. To obtain a more detailed picture of protein unfolding, we also used circular dichroism (CD) to monitor the secondary structure of the proteins.

Protein stability is an important characteristic of protein function. G-protein signaling must be tightly regulated to ensure appropriate responses to extracellular stimuli. Improperly functioning G_α proteins have been implicated in many disease states, including McCune-Albright syndrome, bipolar disorder, and cancer.[21−24] The focus of this study was to compare the stability of WT $G_{i\alpha1}$ and WT $G_{s\alpha}$ from different vantage points: from the inside core of the protein to its surface of the protein and from an overview of the overall secondary structure. Second, we investigated the contribution of each W residue individually and probed the interaction between one of them and the nearby arginine (R) and its effect on protein stability. To elucidate putative folding mechanisms in disease states, we utilized several biophysical techniques to probe the contributions of noncovalent interactions toward the stability of G_α proteins. Computational methods were also used to model the interactions.

2. RESULTS

2.1. Fluorescence Emission Spectra of G_α Subunits.

To calculate melting temperatures in both the active and

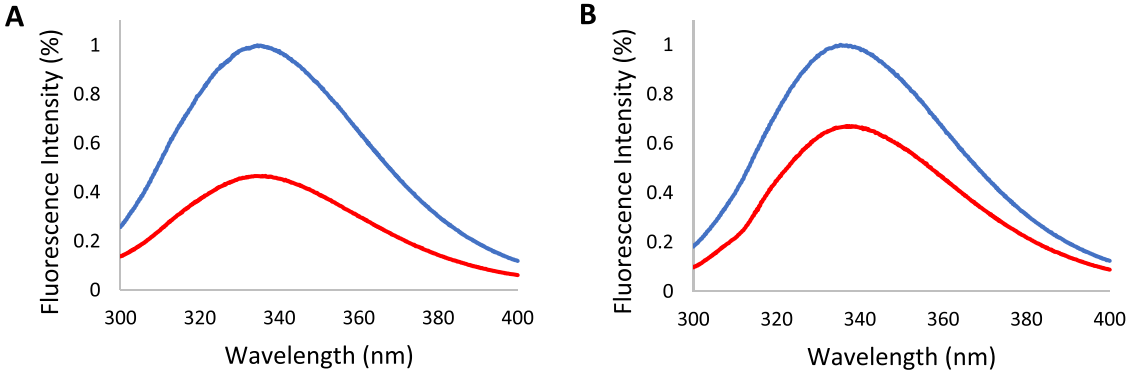

Figure 2. Intrinsic W florescence of WT $G_{i\alpha1}$ proteins. Emission spectra of 0.4 μM WT $G_{i\alpha1}$·Mg^{2+} at 20 °C (blue) and 50 °C (red) in the (A) GDP or (B) GTPγS conformations. Spectra shown were normalized to fluorescence intensities at 450 nm.

DOI: 10.1021/acsomega.8b01174
ACS Omega 2018, 3, 12320−12329

inactive conformations of the WT proteins, we measured the changes in fluorescence intensity, resulting from increases in the solvent exposure of W residues. The amino acid F was chosen as a replacement for W because of its similar structure and size characteristics as well as low quantum yield and distinct λ_{max} values.[19,25]

The fluorescence intensity of WT $G_{i\alpha1}$·GDP at 50 °C decreased by 53% when compared to that observed at 20 °C (Figure 2A), and continued declining until 70 °C, at which point there was no change in intensity and the protein was fully unfolded. A transition midpoint (T_m) of 39 °C was calculated for WT $G_{i\alpha1}$·GDP, and the W mutants in the same conformation were not significantly different from the WT protein (Table 1). For $G_{s\alpha}$ in the GDP conformation, the T_m values for the WT protein were also not significantly different from all W mutants (Table 2).

Table 1. Estimated Melting Temperature (°C) for $G_{i\alpha1}$ Proteins Using Three Spectroscopic Methods[a]

	fluorescence		UV/vis		CD	
$G_{i\alpha1}$ variant	GDP	GTPγS	GDP	GTPγS	GDP	GTPγS
WT	39	49[b]	48	67[b]	44	71[b]
W211F	35	37[c]	47	52[c]	54[c]	57[c]
W131F	38	52[b]	50	54[c]	44	71[b]
W258F	42	59[b,c]	46	63[b,c]	50[c]	68[b]

[a] $n \geq 3$; S.E.M. ≤ 3, for all measurements. [b] $p \leq 0.05$ vs GDP-bound conformation. [c] $p \leq 0.05$ vs WT in the same conformation.

Table 2. Estimated Melting Temperature (°C) for $G_{s\alpha}$ Proteins Using Three Spectroscopic Methods[a]

	fluorescence		UV/vis		CD	
$G_{s\alpha}$ variant	GDP	GTPγS	GDP	GTPγS	GDP	GTPγS
WT	41	39	54	64[b]	52	57[b]
W154F	45	41	53	60[b]	50	57[b]
W234F	40	33[c,b]	53	57[c]	51	53[c]
W277F	45	46[c]	51	60[b]	51[c]	58[b]
W281F	41	40	53	62[b]	54	56[b]

[a] $n \geq 3$; S.E.M. ≤ 3, for all measurements. [b] $p \leq 0.05$ vs GDP-bound conformation. [c] $p \leq 0.05$ vs WT in the same conformation.

For WT $G_{i\alpha1}$·GTPγS, the fluorescence intensity at 50 °C was 33% of that observed at 20 °C, indicating that the active conformation is more stable than the GDP-bound structure (Figure 2B). Apart from the W211F mutant, the T_m values for the other W $G_{i\alpha1}$ mutants in the $G_{i\alpha1}$·GTPγS conformation were also significantly higher than in the GDP conformation (Table 1). Interestingly, the WT $G_{i\alpha1}$·GTPγS showed only a 10 °C increase, whereas the W131F and W258 mutants in the GTPγS conformation were approximately 14 and 17 °C higher than in their respective GDP conformations. The behavior of WT $G_{s\alpha}$·GTPγS and its activated mutants was the opposite of $G_{i\alpha1}$ proteins in the GTPγS conformation. Alignment of the protein sequences indicates that W234F in $G_{s\alpha}$ and W211F in $G_{i\alpha1}$ are both located in the switch II region. The W234F mutant was unique because its T_m value in the GTPγS conformation (33 °C) was significantly lower than in the GDP conformation (40 °C) (Table 2), and the analogous mutation in $G_{i\alpha}$ (W211F) has essentially the same T_m in both the GDP- and GTP-bound forms (Table 1). The T_m values for WT $G_{s\alpha}$ and its W154F, W277F, and W281F mutants in the $G_{s\alpha}$·GTPγS conformation were not significantly different from their GDP counterparts.

2.2. π-Cation Interactions in G_α Subunits. To gain insight into the stability of the switch II region in WT $G_{i\alpha1}$, which co-ordinates with Mg^{2+} and the nucleotide-binding pocket, we monitored the π-cation interaction between R208 and W211 that occurs upon activation from the GDP-bound to the GTPγS conformation. At 20 °C, the λ_{max} position exhibited a red shift of 3.5 nm (Figure 3A), which gradually decreased until 70 °C, at which point the instability of the GDP conformation prevented further measurements (Figure 3B). Similar changes in the value of the λ_{max} position were observed for the WT $G_{s\alpha}$ protein until around 53 °C, where it switched from a red to a blue shift (data not shown).

2.3. UV/Vis Absorption Spectra of G_α Subunits. A useful property of G_α proteins is that W residues move to the hydrophobic core of the protein upon activation.[8] Thus, the spectroscopic and thermal properties of these sites allow for probing the interior of G_α subunits by using fluorescence emission spectroscopy. By contrast, Y residues are predominantly located at the surface of the G_α protein and are therefore useful for determining information on structural changes at or near the exterior of the protein.[8] As the protein unfolds, Y and W residues begin to contribute toward the absorbance. Because W has an absorptivity that is 4 times larger than Y at 280 nm, W would contribute significantly toward the Δ_{abs} as a result of the relative number of Y vs W

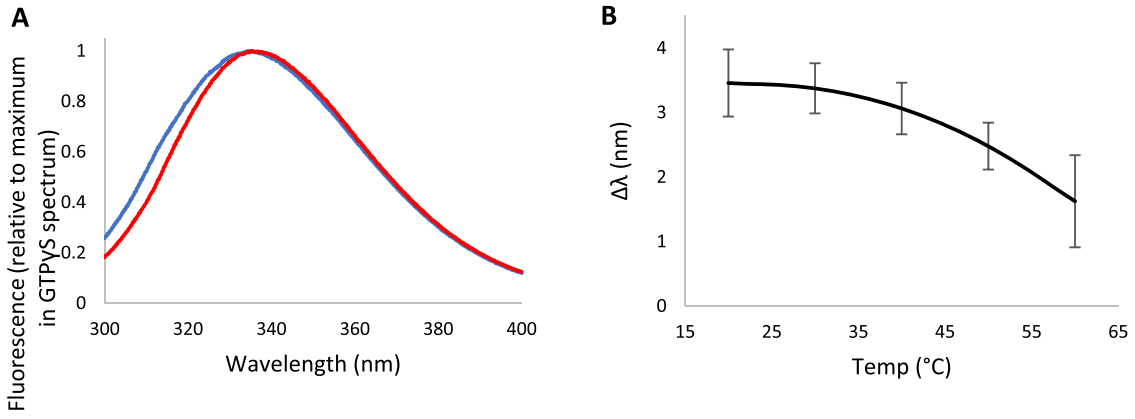

Figure 3. (A) Emission spectra of WT $G_{i\alpha1}$·GDP·Mg^{2+} before (blue) and after (red) activation with GTPγS at 20 °C; (B) temperature variation of the difference between the λ_{max} values of the GTPγS and GDP conformations.

DOI: 10.1021/acsomega.8b01174
ACS Omega 2018, 3, 12320−12329

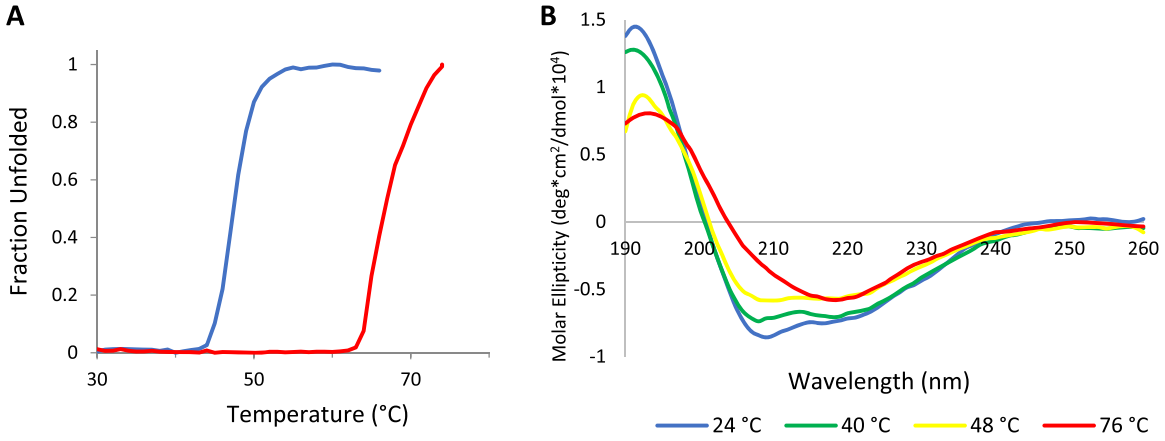

Figure 4. Temperature dependence of the (A) absorption spectra of 2.5 μM WT $G_{i\alpha1}$·Mg^{2+} in the GDP (blue) and GTPγS (red) conformations and of the (B) CD spectra of 1.0 μM WT $G_{i\alpha1}$·GDP·Mg^{2+}.

residues in $G_{i\alpha1}$ (3 vs 13) and in $G_{s\alpha}$ (4 vs 14). In contrast, *F* absorptivity is approximately 30-fold lower than that of Tyr and the λ_{max} is 257 nm, resulting in a negligible contribution toward absorbance at 280 nm.

An increase in absorbance intensity at 280 nm, which was associated to Y and W residues becoming more solvent exposed, was observed at temperatures above 44 °C for WT $G_{i\alpha1}$·GDP. The melting curve for $G_{i\alpha1}$ in the GTPγS form was shifted to the right of the GDP conformation (Figure 4a). A T_m value of 48 °C was calculated for WT $G_{i\alpha1}$·GDP and 54 °C for WT $G_{s\alpha}$·GDP, and for the W mutants, the T_m values were not significantly different from their WT GDP counterparts (Tables 1 and 2). For the GTPγS conformations, the T_m values for WT $G_{i\alpha1}$ and WT $G_{s\alpha}$ were significantly higher than for the GDP counterparts, but were not significantly different for proteins, in which the W residue involved in a π-cation interaction was mutated to F, i.e., W211F for $G_{i\alpha1}$ and W234F for $G_{s\alpha}$ (Tables 1 and 2).

2.4. Temperature Dependence of the Secondary Structure of G_α Subunits. At 20 °C, the CD spectra of WT $G_{i\alpha1}$·GDP (Table 3) and of WT $G_{s\alpha}$·GDP (Table 4) were indicative of proteins that have secondary structures rich in α-helix (40 and 36%, respectively). The percent of α-helix that we observed for WT $G_{i\alpha1}$·GDP was in agreement to that also reported by others using CD (43%), which is less than in the reported structure deposited in the PDB (47%).[8,26] As the temperature increased, the CD absorbance intensity at 190 nm decreased, whereas the minima at 205 nm and 222 nm, which are signatures of α-helix, converged to a new minimum at 215 nm (Figure 4B).

Table 3. Composition of WT $G_{i\alpha1}$ Secondary Structure at Various Temperatures[a,b,c]

	GDP				GTPγS			
T (°C)	α	β	RC[d]	T[d]	α	β	RC[d]	T[d]
20	40	19	26	17	44	12	26	18
40	35	24	24	17	42	14	24	20
52	27	25	27	20	42	13	25	20
64	22	29	29	21	39	16	24	21
80	18	32	28	21	23	26	26	24
92					22	36	51	21

[a] $n \geq 3$; S.E.M ≤ 3. [b] All numbers reported as percentages. [c] Hyphens denote temperatures at which proteins denatured. [d] RC and T stand for random coil and turns.

Table 4. Composition of WT $G_{s\alpha}$ Secondary Structure at Various Temperatures[a,b,c]

	GDP				GTPγS			
T (°C)	α	β	RC[d]	T[d]	α	β	RC[d]	T[d]
20	36	18	33	13	37	16	33	13
40	30	22	34	14	33	20	34	13
52	29	24	34	13	31	20	35	14
64	28	25	34	13	26	24	36	14
80	25	27	35	13	20	27	39	14

[a] $n \geq 3$; S.E.M ≤ 3 for all measurements. [b] All numbers reported as percentages. [c] Hyphens denote temperatures at which proteins denatured. [d] RC and T stand for random coil and turns.

The data in Table 3 indicated that regardless of the conformation, WT $G_{i\alpha1}$ initially was predominantly α-helical, but at higher temperatures, it became increasingly dominated by β-strands and to a lesser extent by random coil. By comparison, WT $G_{s\alpha}$ in both conformations had less α-helical and turn content, but more random coil and had a less dramatic α/β temperature-induced conversion (Table 4). A CD-determined T_m value of 44 °C was calculated for WT $G_{i\alpha1}$·GDP, while the W211F mutant afforded the highest T_m value (Table 1). Experiments with WT $G_{i\alpha1}$·GDP at temperatures greater than 64 °C did not exhibit significant changes in the CD spectra, with the protein eventually precipitating out of solution at 84 °C. Apart from the W211F mutant, WT and W mutants of $G_{i\alpha1}$ in the GTPγS conformation withstood temperatures near 100 °C without precipitation.

At 80 °C, the secondary structure of WT $G_{i\alpha1}$ protein in the active conformation had at least an additional 5% of α-helix content compared to the GDP conformation (Table 3). Except for the $G_{s\alpha}$ W234F and W211F $G_{i\alpha1}$ mutants, the T_m values for the active conformations of WT $G_{s\alpha}$ and the remaining W mutants are significantly higher than for the inactive forms. The CD-determined T_m values for the inactive and active conformations of W234F $G_{s\alpha}$ and W211F $G_{i\alpha1}$ are not significantly different, and the T_m values for the active conformations are significantly lower when compared to the WT proteins (Table 2).

2.5. Refolding. We have also investigated the ability of G_α subunits to refold after completion of the denaturation process. A decrease in temperature was accompanied by an increase in

DOI: 10.1021/acsomega.8b01174
ACS Omega 2018, 3, 12320−12329

fluorescence intensity indicating that the W residues were refolding into hydrophobic environments, as demonstrated for WT $G_{i\alpha1}$·GTPγS (Figure 5A). Refolding WT $G_{i\alpha1}$·GDP from 96 to 4 °C exhibited no significant increase in fluorescence, however, upon renaturation from 48 °C, the observed increase in the fluorescence intensity indicated a refolding recovery of 21% (Figure 5B). When refolding from 32 °C, which is less than the fluorescence-determined T_m value of 39 °C (Table 1), WT $G_{i\alpha1}$·GDP exhibited the largest recovery (72%). Unlike WT $G_{i\alpha1}$·GDP, the GTPγS conformation experienced increases in fluorescence intensity even when refolding was initiated from 96 °C, i.e., at temperatures larger than the T_m (Figure 5B and Table 1). These observations demonstrate that the ability of G_α subunits to refold is conformation-dependent. Although this is the case for both G_α proteins, WT $G_{i\alpha1}$ was able to recover the most folded structure compared to WT $G_{s\alpha}$ (spectra not shown). Such traits were drawn out by fluorescence spectra of WT $G_{i\alpha1}$·GTPγS that revealed a 76% recovery after denaturation at temperatures up to 70 °C. By contrast, we found that WT $G_{s\alpha}$·GTPγS only recovered 30% of its folded structure after denaturation at temperatures ≤ 84 °C. In addition, WT $G_{s\alpha}$·GDP precipitated at temperatures less than 80 °C during renaturation.

CD was also used to monitor the reversibility of protein unfolding. As shown in Figure 5C, when WT $G_{i\alpha1}$·GDP was cooled from 76 to 20 °C, there was a concomitant increase in the spectral intensity at 190 nm and a decrease at 222 nm. Spectral deconvolution showed that at 80 °C, WT $G_{i\alpha1}$·GDP consisted primarily of 18% α-helices and 32% β-sheets (Table 3), but protein refolding back to 20 °C increased the α-helical content to 31%, whereas the percentage of β-sheets decreased to 18%. Terminating the denaturation process at 52 °C rather than at 76 °C resulted in recovery of 88% of the original α-helical structure. Similar effects were observed with WT $G_{i\alpha1}$·GTPγS. Although this conformation was more resistant to unfolding as evidenced by an initial 44% α-helical content at 20 °C (Table 3), 93% of which was recovered when refolding from 76 to 20 °C.

To ascertain whether the partial recovery of structural refolding described above translated into a gain in protein activity, we investigated the kinetics of GTPγS binding at several temperatures (Figure 6). Because of differences in protein stability, the decrease in fluorescence intensity for the protein in the inactive conformation is larger than in the active

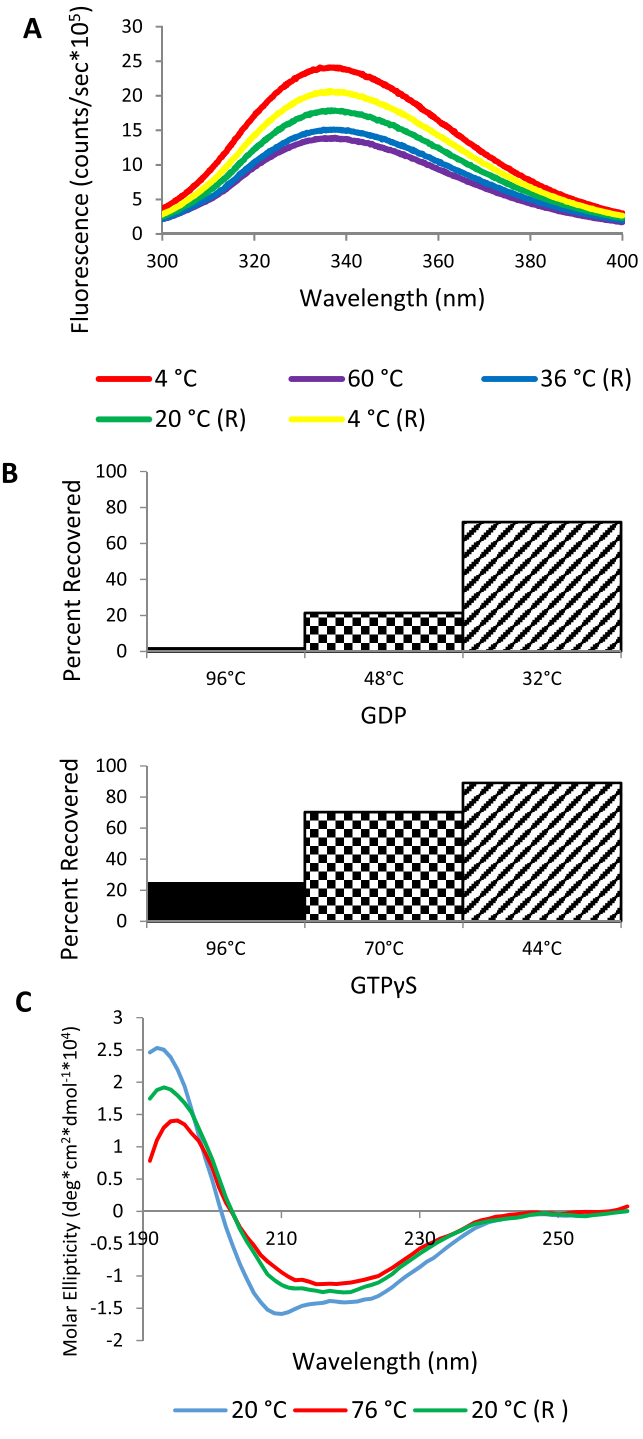

Figure 5. (A) Refolding of WT $G_{i\alpha1}$·GTPγS as monitored via emission spectroscopy. Spectra shown were scaled to fluorescence intensities at 450 nm. (B) Percent fluorescence recovered after refolding of WT $G_{i\alpha1}$. Temperatures denote the maximum temperatures to which protein solutions were exposed before cooling. (C) Probing of denaturation and refolding of WT $G_{i\alpha1}$·GDP by circular dichroism. R represents refolded $G_{i\alpha1}$.

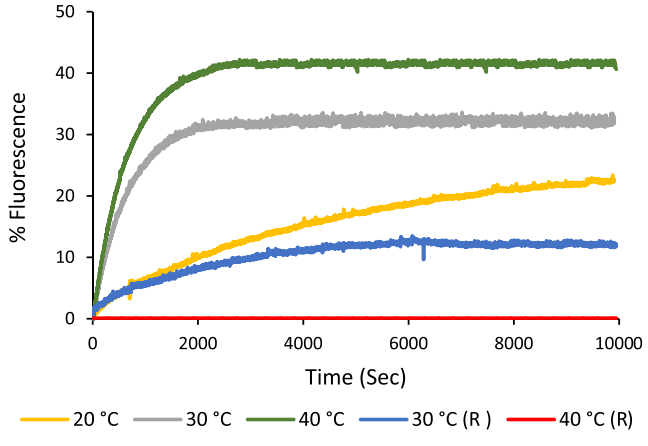

Figure 6. Temperature dependence of GTPγS binding to WT $G_{i\alpha1}$·GDP as monitored by time-based tryptophan fluorescence emission assays. R denotes traces from protein solutions that were heated to the higher temperature shown and then cooled to 20 °C. % fluorescence = $((F_o - F_i)/F_i) \times 100$, where F_i and F_o are the fluorescence intensities in arbitrary units at the start of GTPγS activation and at time t °C.

DOI: 10.1021/acsomega.8b01174
ACS Omega 2018, 3, 12320−12329

Table 5. Interaction Energies between R208 and W211 for $G_{i\alpha1}$ WT[a,b]

	GDP		GTP		Δ (GTP-GDP)	
temperature	electrostatic	vdW	electrostatic	vdW	electrostatic	vdW
37 °C	−0.96	−3.38	−2.85	−4.38	−1.89	−1.00
50 °C	0.33	−2.16	−1.38	−4.61	−1.71	−2.45
Δ (50−37 °C)	1.29	1.22	1.47	−0.23	0.18	−1.45

[a]S.E.M. ≤ 3.0. [b]Values are in kcal/mol.

conformation (Figure 2). Consequently, normalizing the initial fluorescence intensities of WT $G_{i\alpha1}$ in the GDP conformation at 40 and 30 °C to the same value accounts for the maximal fluorescence intensity observed upon GTPγS binding being the largest at 40 °C (Figure 6). Heating WT $G_{i\alpha1}$ to 30 °C followed by cooling to 20 °C resulted in approximately 45% recovery of GTPγS binding, but when the protein was heated to 40 °C and then cooled to 20 °C, no GTPγS binding was found. As shown in Table 1, the melting temperature of WT $G_{i\alpha1}$ in the GDP conformation as measured by fluorescence is 39 °C, indicating that WT $G_{i\alpha1}$·GDP is unstable at 40 °C for GDP → GTPγS exchange to occur. In summary, these findings indicate that G_α subunits have the ability to partially regain GTPγS binding activity (Figure 6) and that to some extent, refold the structure as demonstrated by our data obtained with two independent spectroscopic methods (fluorescence and circular dichroism; Figure 5). To the best of our knowledge, this is the first time that a regain of function after refolding was reported for G_α subunits.

3. DISCUSSION

Protein stability is critical for biological function. Our study focused on characterizing the noncovalent interactions that contribute to the stability of G_α proteins and to the reformation of the protein structure after unfolding. Surprisingly, given the importance of G_α proteins, there have been few studies of their stabilities.[27−29] In vivo, chaperones contribute toward protein stability. With respect to G_α subunits, the Ric-8A and Ric-8B chaperones play a part in the folding of nascent $G_{i\alpha1}$ and $G_{s\alpha}$.[30]

A comparison of the WT $G_{i\alpha1}$ crystal structures in the GDP and GTPγS conformations reveals that the GDP-bound structure has a larger surface area than the active GTPγS conformation.[5,8] One would predict that compared to the GDP form, a denser folding profile for the GTPγS conformation of WT $G_{i\alpha1}$ would result in a more stable structure, as evidenced by the higher T_m values calculated from fluorescence emission, combined Y and W absorption, and CD spectra as well as from the larger interaction energies calculated for the GTP-bound protein (Tables 1 and 5). This conclusion is also supported by solvent accessible surface area (SASA) calculations for WT $G_{i\alpha1}$ indicating that protein activation resulted in a 2.6% decrease in overall solvent exposure (19 520 Å^2 for GDP-bound protein vs 19 010 Å^2 for the active conformation). Therefore, WT $G_{i\alpha1}$·GTPγS is more stable, thus requiring more energy to unfold.

Utilizing W → F single-point mutations, we followed the unfolding by measuring the temperature dependence of the fluorescence emission spectra of nine G_α proteins (WT and three W mutants of $G_{i\alpha1}$ and WT and four W mutants of $G_{s\alpha}$) in the inactive GDP and active GTPγS conformations. Because burial of W residues in hydrophobic pockets is known to result in an increase in ΔF_{max}, protein unfolding is accompanied by a decrease in fluorescence intensity.[31] In the GDP forms (Table 1), the fluorescence-measured T_m values for WT $G_{i\alpha1}$ were not significantly different ($p < 0.1$) from its W mutants. Except for the W211F mutant, the T_m values were, however, significantly smaller than for the active WT $G_{i\alpha1}$, W131F, and W258F proteins ($p < 0.01$). The GTPγS conformation of the W211F mutant proved to be the least stable of all of the active $G_{i\alpha1}$ proteins and displayed a fluorescence-derived T_m value similar to its GDP conformation (Table 1), which is the opposite of the general trend of higher melting temperatures observed for the GTPγS conformations. The difference in the interaction energies for the GDP and GTP found during the molecular dynamics simulations was smaller for the W211F variant than for the WT, which might contribute to the active conformation of this mutant being less stable.

Unlike WT $G_{i\alpha1}$, for which crystal structures are known for the inactive and active conformations, only the structure of WT $G_{s\alpha}$·GTPγS has been published, precluding an explanation of protein stability based on compactness or differences in GTP and GDP interaction energies with the protein.[5,8,32] The fluorescence-derived data in Table 2 indicate that WT $G_{s\alpha}$ and its mutants do not follow the same folding pattern as for $G_{i\alpha1}$. For T_m values calculated from fluorescence spectra, there is no significant difference between the active and inactive conformations of WT $G_{s\alpha}$ and of its W154F, W277F, and W281F mutants suggesting that with the exception of W234F $G_{s\alpha}$, stability of the protein structure around the W residues in $G_{s\alpha}$ is different from $G_{i\alpha1}$. Figure 7 shows that at room temperature, the ΔF_{max} values were significantly lower for WT $G_{s\alpha}$ relative to WT $G_{i\alpha1}$. Since ΔF_{max} is a result of W movement, this trend suggests that after activation a smaller displacement of the W residues occurs in $G_{s\alpha}$ compared to $G_{i\alpha1}$. Therefore, unlike WT $G_{i\alpha1}$, the W residues in the GDP conformation of WT $G_{s\alpha}$ are relatively protected in hydrophobic environments, presumably accounting for the insignificant difference between the T_m values from WT $G_{s\alpha}$·GTPγS and WT $G_{s\alpha}$·GDP (Table 2). The insignificant differences between the T_m values from the active and inactive conformations of the W154F, W277F, and W281F mutants of $G_{s\alpha}$ are likely to have the same origin.

The W211F mutant of $G_{i\alpha1}$ and the W234F mutant of $G_{s\alpha}$ do not show detectable changes in ΔF_{max} (Figure 7, panels A and B). The W211 residue in WT $G_{i\alpha1}$ has been shown to have the largest difference in solvent accessibility between the inactive and active conformations and therefore contributes the most toward ΔF_{max}.[19] Not surprisingly, for the W211F mutant of $G_{i\alpha1}$, no ΔF_{max} is observed (Figure 7B). Similarly, the W234 residue in $G_{s\alpha}$ likely undergoes a similar large decrease in solvent accessibility during the course of the conformational change, as evidenced by the negligible ΔF_{max} observed in the W234F mutant (Figure 7A). The fluorescence-derived T_m values for the W211F mutant of $G_{i\alpha1}$ are not statistically different in the two conformations (Table 1) presumably because of the absence of the W211-R208 cation−π

DOI: 10.1021/acsomega.8b01174
ACS Omega 2018, 3, 12320−12329

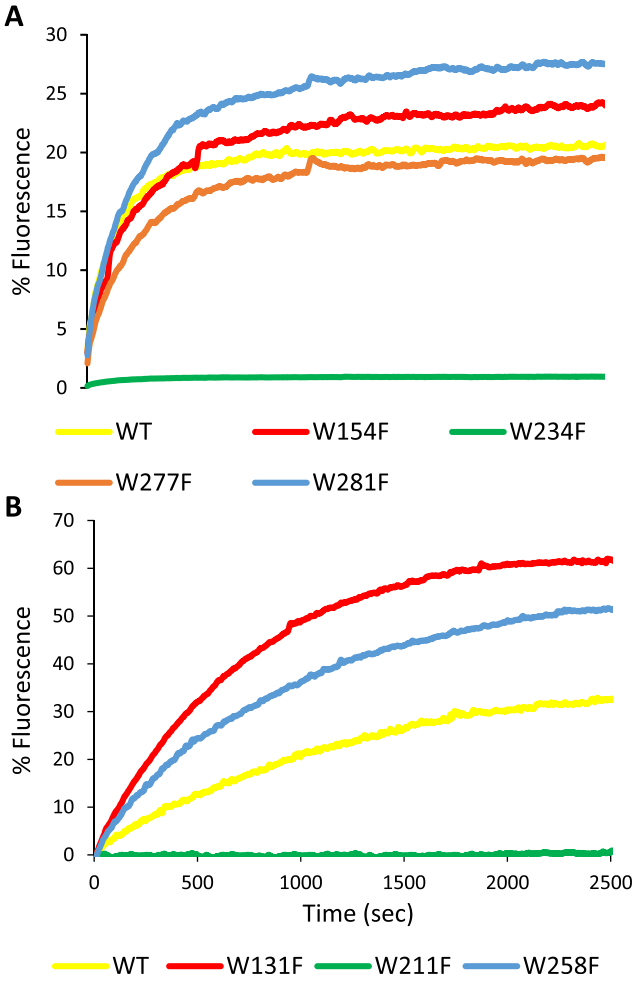

Figure 7. Time-based emission assay monitoring percent change in intrinsic tryptophan fluorescence of (A) WT $G_{s\alpha}$ and (B) WT $G_{i\alpha1}$ and their respective Trp mutants after the addition of GTPγS. % fluorescence was calculated in the same manner as for Figure 6.

interaction. Interestingly, the T_m value for the W234F mutant is significantly lower than for WT $G_{s\alpha}$ (Table 2).

The secondary structure of WT $G_{i\alpha1}$ proved to be the most stable in its GTPγS form relative to the GDP conformation (Table 1). At 20 °C and upon binding of GTPγS, we identified a 4% increase in the α-helical content of WT $G_{i\alpha1}$ (Table 3), but not for WT $G_{s\alpha}$ (Table 4). Activation of WT $G_{i\alpha1}$ creates a hydrophobic pocket via folding of the switch regions, resulting in a protein that has an ordered secondary structure with an increased α-helical content.[4,8] The smaller ΔF_{max} observed for activation of WT $G_{s\alpha}$ relative to WT $G_{i\alpha1}$ (Figure 7) may be related to a smaller change in the secondary structure of WT $G_{s\alpha}$. In either conformation, as the temperature increased, the α-helical content of both WT G_α proteins was reduced and the subunits became richer in β-sheet while the random coil and turn structures were not altered significantly from the native form. We have done molecular dynamics simulations of the thermal unfolding of the monomeric G_α proteins and have not observed an increase in β-sheet, although the amount of α-helix decreased. These simulations may indicate that the β-sheet increase is due to aggregation.

A shift in secondary structure from primarily α-helices to β-sheets poses an increased risk for protein aggregation that may lead to amyloidogenesis.[16] Amyloid fibril formation occurs when unfolded, native-like proteins aggregate into long filaments of packed β-sheets.[33−35] Many debilitating neurodegenerative diseases, such as Parkinson's, Creutzfeldt-Jakob's, and Alzheimer's, have been proposed to arise from the accumulation of amyloid fibrils in the brain or in the central nervous system.[16] In vitro studies have shown that it is not uncommon for proteins to form amyloid fibrils under denaturing conditions.[36,37] Furthermore, fibril formation has been shown to inhibit refolding into the native conformation.[38]

The absorbance assays helped visualize the global unfolding of G_α subunits from another perspective. The T_m values for WT $G_{i\alpha1}$ that were calculated from the absorbance of Y and W residues correlate to the unfolding process (Figure 4A). UV/vis experiments with $G_{i\alpha1}$ showed that the protein surface in the GTPγS conformation to be significantly more stable than the W microenvironments, whereas the CD-determined values indicated that the surface unfolded before the secondary structure (Table 1). In the case of WT $G_{s\alpha}$·GTPγS, the UV/vis-calculated T_m value was the highest compared to those derived from the other measurements, indicating that the surface of the WT $G_{s\alpha}$ is the last to unfold (Table 2). In the W211F mutant of $G_{i\alpha1}$ and in the W234F mutant of $G_{s\alpha}$, no significant difference between the T_m values was observed upon activation. One possibility is that π−cation interactions, involving W211 in $G_{i\alpha1}$ and W234 in $G_{s\alpha}$, affect unfolding proximal to Y and W residues. π−cation interactions are found in many proteins.[39,40] They are known to contribute significantly to thermal stability.[41,42] The average energy for W−cation interactions is −2.9 ± 1.4 kcal/mol.[41,42] For the W154F, W277F, and W281F mutants of $G_{s\alpha}$, the UV/vis-determined T_m values were significantly higher for the active conformations. For $G_{i\alpha1}$, however, only the W258F mutant was stabilized, suggesting a distinct folding pattern for the two G_α subunits in each conformation.

We have examined the thermal denaturation of the G_α proteins using three different optical probes: absorbance, fluorescence, and CD. These probes primarily measure changes in the environments of Y residues or W residues or the secondary structure, respectively. Since they give different T_m values for the same protein (Tables 1 and 2), the denaturation of both G_α proteins appears to be multistate rather than two state.[43] The differences in T_m values in G_α that were observed by different methods may be rationalized via an analysis of the hydrophobic interactions, which are fundamental folding determinants for all proteins. Noncovalent interactions underpin the driving forces in protein folding. The observed T_m values suggest that denaturation of the active conformation of $G_{i\alpha1}$ starts near W131 and W258 microenvironments, and then propagates outward through the protein surface where the Y residue proximal to W258 is located, and at this point of unfolding leaving the secondary structure intact. Additional heating results in the conversion of α-helixes into β-sheets and random coil, possibly involving aggregation until precipitation occurs. In contrast, denaturation of the active conformation of $G_{s\alpha}$ initiates equally around all W residues, continuing to the secondary structure and is completed near the Y residues.

The robustness and resistance of a protein to misfolding minimize the chances for disease. The reversibility of folding observed with WT $G_{i\alpha1}$ via fluorescence emission and CD (Figure 5a,c) can therefore shed important light on the misfolding of G_α subunits. During the course of denaturation, a protein may develop multiple intermediate conformations, or

DOI: 10.1021/acsomega.8b01174
ACS Omega 2018, 3, 12320−12329

molten globule states, which are reflected by the different T_m values obtained by the three techniques.[44] The fluorescence spectra monitored, to a significant degree, the polarity changes surrounding the W sites. Oscillations of the nonpolar side chains at these sites would generate molten globules with relatively low thermal energies. These movements would account for the lower T_m values calculated from fluorescence measurements, compared to those obtained with the other two spectroscopic probes. Multiple Y residues, which may be involved in hydrogen bonding, are distributed throughout G_α. Once protein unfolding is initiated, molten globule states that are populated will exhibit diminished secondary structure, which is determined by hydrogen bonding. The additional contribution of hydrogen bonding associated with Y microenvironments and secondary structure relative to primarily hydrophobic interactions present in the vicinities of W residues may explain the higher T_m values measured from Y absorption and CD spectra.

Previous work by Najor et al. and Hamm and co-workers showed that W211 forms a π−cation interaction with R208 in WT $G_{i\alpha1}$·GTPγS, as evidenced by a red shift of 2.5 nm in the λ_{max} value (Figure 3a).[19,20] Molecular dynamic simulations predict that the conformational change from the inactive to the active conformation results in an increase in the electrostatic interaction between W211 and R208 from −0.96 to −2.85 kcal/mol, which is consistent to the higher stability seen in the active conformation (Table 5). Thus, stronger ligand−protein interactions would help stabilize the GTPγS-bound structure. Molecular dynamics studies showed that the interaction energy between GTP and $G_{i\alpha1}$ at 323 K (−621.7 kcal/mol) indicated that GTP binds more tightly than GDP (−494.4 kcal/mol). This binding energy partially may explain why the GTP-bound structure refolds better.

An increase in temperature at which the simulation was conducted (37 → 50 °C) resulted in weakening of the W211-R208 π−cation interaction, which is supported by the observed decrease in the $\Delta\lambda_{max}$ (Figure 3b). The increased van der Waals interactions calculated at higher temperatures may be associated with these residues swinging into more hydrophilic environments upon unfolding. This conclusion is supported by a blue (rather than red) shift observed upon the GTPγS activation of $G_{s\alpha}$ at temperatures higher than 53 °C. For the W211F mutant of $G_{i\alpha1}$, there was no significant difference between the T_m values from the active and inactive conformations further suggesting that the π−cation interaction is important for the structural integrity of $G_{i\alpha1}$.

This study underscores the importance of π−cation interactions toward protein stability. The disruption of these noncovalent interactions may lead to significant decreases in the stabilities for the active conformations of G_α subunits and could promote improper folding. Mutations of the arginine residue involved in the π−cation interaction have been identified in the R208Q $G_{i\alpha1}$ and in the R231H $G_{s\alpha}$ oncogenes and are thought to have similar characteristics as the W mutants.[23] The loss of the π−cation interaction could translate into changes in structure−function relationships by disrupting the signaling cascade for cAMP. Future studies will focus on the effect of these mutations on the structure and function of oncogenic G_α subunits.

4. EXPERIMENTAL SECTION

4.1. Expression and Protein Purification. $G_{\alpha i1}$ and $G_{s\alpha}$ were obtained and purified as previously described.[45] Single-point W mutants of $G_{\alpha i1}$ and $G_{s\alpha}$ were prepared by site-directed mutagenesis using a kit provided by Stratagene (La Jolla, CA). After purification on a Ni^{2+} affinity column followed by a Superdex 200 pg size exclusion column, the purity of GDP-bound G_α proteins was found to be greater than 95% as estimated by sodium dodecyl sulfate−polyacrylamide gel electrophoresis. Protein was stored at −80 °C in 20 mM Tris, pH 8.0 buffer containing 10% (v/v) glycerol, and 1 mM dithiothreitol (DTT).

4.2. Fluorescence Measurements of Protein Activation. Experiments were performed with a PTI QuantaMaster fluorimeter (Photon Technologies, Inc., Mirmingham, NJ). Indirect activity assays were conducted with excitation and emission wavelengths set at 280 and 340 nm, respectively. Assays were initiated after 60 s by addition of 20 μM of GTPγS to preincubated 400 nM G_α·GDP protein samples in buffer containing 50 mM *N*-(2-hydroxyethyl)piperazine-*N*′-ethanesulfonic acid, pH 7.5, 2 mM $MgSO_4$, and 1 mM DTT, and was monitored for 3 h at 25 °C. The GDP- and GTPγS-bound proteins that were characterized by the activity assays were used in the following denaturation studies.

4.3. Fluorescence-Measured Protein Denaturation. Emission spectra for both GDP- and GTPγS-bound proteins were recorded over the wavelength range of 300−400 nm with the excitation wavelength set at 280 nm. Signal integration time was 0.2 s with the bandpass for excitation and for emission set at 5 nm. The denaturation experiments started at a temperature of 4 °C followed by 4 °C increments and concluding at the highest temperature before precipitation occurred. There was a 2 min equilibration period at each set temperature. All T_m values were calculated from fluorescence intensities at the spectral λ_{max} positions for the selected temperatures, using methods adapted from those previously described.[46]

4.4. UV/Vis-Measured Protein Denaturation. The environments of Y (and to a lesser extent W) residues in G_α proteins were monitored on a Hewlett Packard UV/vis spectrophotometer. All samples contained 50 mM Tris, pH 7.5, 1 μM G_α·GDP protein, 1 mM DTT, and 2 mM $MgSO_4$. Prior to initiating the experiments, samples were incubated with their respective nucleotide, 2.5 μM G_α·GDP or 20 μM GTPγS, at room temperature for 1 h. The temperature was increased from 20 to 80 °C, at 0.3 °C/min over 180 min. For each temperature studied, samples were equilibrated for 1 min, and the absorbance was monitored in the wavelength range of 220−300 nm. All melting temperatures were calculated from the absorbance values at 280 nm for the different temperatures, using methods previously described.[47]

4.5. CD-Measured Protein Denaturation. Experiments were performed using an Olis DSM 20 circular dichroism spectrophotometer. All samples were measured in a cylindrical quartz cuvette with a 1 mm pathlength and contained either 3 μM G_α·GDP or 24 μM G_α·GTPγS, in 10 mM phosphate, pH 7.5 buffer, 1 mM DTT, and 2 mM $MgSO_4$. Data were collected at 150 V every 1 nm in the wavelength range of 190−260 nm. The temperature was increased from 20 to 100 °C at 4 °C increments with an incubation time of 3 min at each temperature studied. The CONTIN LL algorithm was used to deconvolute the spectra using reference sets with denatured proteins to calculate the percent of each type of secondary structure and T_m values for each protein studied.[48−50]

4.6. Refolding of G_α Subunits. To test whether unfolding of G_α proteins was reversible, fluorescence emission scans and

DOI: 10.1021/acsomega.8b01174
ACS Omega 2018, 3, 12320−12329

CD spectrophotometry were used. Once spectra from the final temperature of an unfolding experiment were obtained, G_{α} samples were cooled down in 8 °C increments and incubation times remained the same as indicated above for each respective technique. Final temperatures varied depending on aggregation and ability to refold. All renaturation experiments were stopped at 4 °C for fluorescence measurements and at 20 °C for CD experiments.

4.7. Molecular Modeling. The co-ordinates of GDP (1BOF[8]) and GTPγS (1GIA[5]) derivatives of $G_{i\alpha1}$ and GTPγS of $G_{s\alpha}$ (1AZT[32]) were downloaded from the Protein Data Bank (PDB[51]). Missing loops in the $G_{i\alpha1}$ structures were modeled using Swiss Model[52] and the corresponding transducin structures (1TAG,[53] 1TAD,[54] and 1TND[55]). The simulations were done using procedures previously described.[19] Unrestrained dynamics was run for 14 ns before the data were acquired for an additional 1 ns. The simulations were done at 37 °C (310 K) and 50 °C (328 K). These data were then used in the analyses. The initial W point mutation models were generated using VMD[56] and then subjected to the same equilibration procedure as the wild-type structures. All molecular graphic diagrams were generated using VMD.[56] Pairwise van der Waals and electrostatic interaction energies were calculated using NAMD.[57] The solvent accessible surface area (SASA) was measured with the SASA routine in VMD.[56] The SASA values and the van der Waals and electrostatic energy values presented in Table 5 were calculated for the final 1 ns in each simulation and then averaged.

AUTHOR INFORMATION

Corresponding Author

*E-mail: dfreita@luc.edu.

ORCID

Duarte Mota de Freitas: 0000-0001-9303-6173

Author Contributions

†M.N. and B.D.L. contributed equally to this work.

Notes

The authors declare no competing financial interest.

ACKNOWLEDGMENTS

This work received funding support from the National Institutes of Health (R15GM112025). We are grateful for the assistance from Iva Gomeli, Colin Senfelds, and Stephen Chukwelebe.

REFERENCES

(1) Sprang, S. R. Invited review: Activation of G proteins by GTP and the mechanism of G_{α}-catalyzed GTP hydrolysis. *Biopolymers* **2016**, *105*, 449−462.

(2) Oldham, W. M.; Hamm, H. E. Heterotrimeric G protein activation by G-protein-coupled receptors. *Nat. Rev. Mol. Cell Biol.* **2008**, *9*, 60−71.

(3) Oldham, W. M.; Hamm, H. E. Structural basis of function in heterotrimeric G proteins. *Q. Rev. Biophys.* **2006**, *39*, 117−166.

(4) Mixon, M. B.; Lee, E.; Coleman, D. E.; Berghuis, A. M.; Gilman, A. G.; Sprang, S. R. Tertiary and quaternary structural changes in $G_{i\alpha1}$ induced by GTP hydrolysis. *Science* **1995**, *270*, 954−960.

(5) Coleman, D. E.; Berghuis, A. M.; Lee, E.; Linder, M. E.; Gilman, A. G.; Sprang, S. R. Structures of active conformations of $G_{i\alpha1}$ and the mechanism of GTP hydrolysis. *Science* **1994**, *265*, 1405−1412.

(6) Tesmer, J. J.; Sunahara, R. K.; Gilman, A. G.; Sprang, S. R. Crystal structure of the catalytic domains of adenylyl cyclase in a complex with $G_{s\alpha}$·GTPγS. *Science* **1997**, *278*, 1907−1916.

(7) Bae, H.; Anderson, K.; Flood, L. A.; Skiba, N. P.; Hamm, H. E.; Graber, S. G. Molecular determinants of selectivity in 5-hydroxytryptamine1B receptor-G protein interactions. *J. Biol. Chem.* **1997**, *272*, 32071−32077.

(8) Coleman, D. E.; Sprang, S. R. Crystal structures of the G protein $G_{i\alpha1}$ complexed with GDP and Mg^{2+}: A crystallographic titration experiment. *Biochemistry* **1998**, *37*, 14376−14385.

(9) Pace, C. N.; Scholtz, J. M.; Grimsley, G. R. Forces stabilizing proteins. *FEBS Lett.* **2014**, *588*, 2177−2184.

(10) Englander, S. W.; Mayne, L. The nature of protein folding pathways. *Proc. Natl. Acad. Sci. U.S.A.* **2014**, *111*, 15873−15880.

(11) Dill, K. A.; MacCallum, J. L. The protein-folding problem, 50 years on. *Science* **2012**, *338*, 1042−1046.

(12) Schiffrin, B.; Brockwell, D. J.; Radford, S. E. Outer membrane protein folding from an energy landscape perspective. *BMC Biol.* **2017**, *15*, 123.

(13) Baldwin, R. L.; Rose, G. D. Molten globules, entropy-driven conformational change and protein folding. *Curr. Opin. Struct. Biol.* **2013**, *23*, 4−10.

(14) Shortle, D. The denatured state (the other half of the folding equation) and its role in protein stability. *FASEB J.* **1996**, *10*, 27−34.

(15) Bhattacharyya, S.; Varadarajan, R. Packing in molten globules and native states. *Curr. Opin. Struct. Biol.* **2013**, *23*, 11−21.

(16) Selkoe, D. J. Folding proteins in fatal ways. *Nature* **2003**, *426*, 900−904.

(17) Higashijima, T.; Ferguson, K. M.; Smigel, M. D.; Gilman, A. G. The effect of GTP and Mg^{2+} on the GTPase activity and the fluorescent properties of G_o. *J. Biol. Chem.* **1987**, *262*, 757−761.

(18) Higashijima, T.; Ferguson, K. M.; Sternweis, P. C.; Ross, E. M.; Smigel, M. D.; Gilman, A. G. The effect of activating ligands on the intrinsic fluorescence of guanine nucleotide-binding regulatory proteins. *J. Biol. Chem.* **1987**, *262*, 752−756.

(19) Najor, M. S.; Olsen, K. W.; Graham, D. J.; Mota de Freitas, D. Contribution of each Trp residue toward the intrinsic fluorescence of the $G_{i\alpha1}$ protein. *Protein Sci.* **2014**, *23*, 1392−1402.

(20) Hamm, H. E.; Meier, S. M.; Liao, G.; Preininger, A. M. Trp fluorescence reveals an activation-dependent cation-π interaction in the switch II region of $G_{\alpha i}$ proteins. *Protein Sci.* **2009**, *18*, 2326−2335.

(21) Berrettini, W. H.; Vuoristo, J.; Ferraro, T. N.; Buono, R. J.; Wildenauer, D.; Ala-Kokko, L. Human G(olf) gene polymorphisms and vulnerability to bipolar disorder. *Psychiatr. Genet.* **1998**, *8*, 235−238.

(22) Weinstein, L. S.; Shenker, A.; Gejman, P. V.; Merino, M. J.; Friedman, E.; Spiegel, A. M. Activating mutations of the stimulatory G protein in the McCune-albright syndrome. *N. Engl. J. Med.* **1991**, *325*, 1688−1695.

(23) Dorsam, R. T.; Gutkind, J. S. G-protein-coupled receptors and cancer. *Nat. Rev. Cancer* **2007**, *7*, 79−94.

(24) O'Hayre, M.; Vazquez-Prado, J.; Kufareva, I.; et al. The emerging mutational landscape of G proteins and G-protein-coupled receptors in cancer. *Nat. Rev. Cancer* **2013**, *13*, 412−424.

(25) Vivian, J. T.; Callis, P. R. Mechanisms of tryptophan fluorescence shifts in proteins. *Biophys J.* **2001**, *80*, 2093−2109.

(26) Tanaka, T.; Kohno, T.; Kinoshita, S.; et al. Alpha helix content of G protein α subunit is decreased upon activation by receptor mimetics. *J. Biol. Chem.* **1998**, *273*, 3247−3252.

(27) Streiff, J.; Warner, D. O.; Klimtchuk, E.; Perkins, W. J.; Jones, K.; Jones, K. A. The effects of hexanol on $G_{i\alpha1}$ subunits of heterotrimeric G proteins. *Anesth. Analg.* **2004**, *98*, 660−667.

(28) Northup, J. K.; Smigel, M. D.; Sternweis, P. C.; Gilman, A. G. The subunits of the stimulatory regulatory component of adenylate cyclase. resolution of the activated 45,000-dalton (α) subunit. *J. Biol. Chem.* **1983**, *258*, 11369−11376.

(29) Johnston, C. A.; Afshar, K.; Snyder, J. T.; et al. Structural determinants underlying the temperature-sensitive nature of a G_{α} mutant in asymmetric cell division of *Caenorhabditis elegans*. *J. Biol. Chem.* **2008**, *283*, 21550−21558.

(30) Chan, P.; Thomas, C. J.; Sprang, S. R.; Tall, G. G. Molecular chaperoning function of ric-8 is to fold nascent heterotrimeric G

DOI: 10.1021/acsomega.8b01174
ACS Omega 2018, 3, 12320−12329

protein α subunits. *Proc. Natl. Acad. Sci. U.S.A.* **2013**, *110*, 3794−3799.
(31) Stryer, L. Fluorescence spectroscopy of proteins. *Science* **1968**, *162*, 526−533.
(32) Sunahara, R. K.; Tesmer, J. J.; Gilman, A. G.; Sprang, S. R. Crystal structure of the adenylyl cyclase activator $G_{sα}$. *Science* **1997**, *278*, 1943−1947.
(33) Chiti, F.; Dobson, C. M. Protein misfolding, amyloid formation, and human disease: A summary of progress over the last decade. *Annu. Rev. Biochem.* **2017**, *86*, 27−68.
(34) Chandel, T. I.; Zaman, M.; Khan, M. V.; et al. A mechanistic insight into protein-ligand interaction, folding, misfolding, aggregation and inhibition of protein aggregates: An overview. *Int. J. Biol. Macromol.* **2018**, *106*, 1115−1129.
(35) Morris, A. M.; Watzky, M. A.; Finke, R. G. Protein aggregation kinetics, mechanism, and curve-fitting: A review of the literature. *Biochim. Biophys. Acta.* **2009**, *1794*, 375−397.
(36) Dao, K. K.; Pey, A. L.; Gjerde, A. U.; et al. The regulatory subunit of PKA-I remains partially structured and undergoes β-aggregation upon thermal denaturation. *PLoS One* **2011**, *6*, No. e17602.
(37) Fändrich, M.; Forge, V.; Buder, K.; Kittler, M.; Dobson, C. M.; Diekmann, S. Myoglobin forms amyloid fibrils by association of unfolded polypeptide segments. *Proc. Natl. Acad. Sci. U.S.A.* **2003**, *100*, 15463−15468.
(38) Plaza del Pino, I. M.; Ibarra-Molero, B.; Sanchez-Ruiz, J. M. Lower kinetic limit to protein thermal stability: A proposal regarding protein stability in vivo and its relation with misfolding diseases. *Proteins* **2000**, *40*, 58−70.
(39) Gallivan, J. P.; Dougherty, D. A. Cation-π interactions in structural biology. *Proc. Natl. Acad. Sci. U.S.A.* **1999**, *96*, 9459−9464.
(40) Dougherty, D. A. The cation-π interaction. *Acc. Chem. Res.* **2013**, *46*, 885−893.
(41) Tayubi, I. A.; Sethumadhavan, R. Nature of cation-π interactions and their role in structural stability of immunoglobulin proteins. *Biochemistry* **2010**, *75*, 912−918.
(42) Prajapati, R. S.; Sirajuddin, M.; Durani, V.; Sreeramulu, S.; Varadarajan, R. Contribution of cation-π interactions to protein stability. *Biochemistry.* **2006**, *45*, 15000−15010.
(43) Senisterra, G.; Chau, I.; Vedadi, M. Thermal denaturation assays in chemical biology. *Assay Drug Dev. Technol.* **2012**, *10*, 128−136.
(44) Fink, A. L.; Oberg, K. A.; Seshadri, S. Discrete intermediates versus molten globule models for protein folding: Characterization of partially folded intermediates of apomyoglobin. *Fold Des.* **1998**, *3*, 19−25.
(45) Lee, E.; Linder, M. E.; Gilman, A. G. Expression of G-protein α subunits in *Escherichia coli*. *Methods Enzymol.* **1994**, *237*, 146−164.
(46) Brandts, J. F. The thermodynamics of protein denaturation. I. the denaturation of chymotrypsinogen. *J. Am. Chem. Soc.* **1964**, *86*, 4291−4301.
(47) Olsen, K. W. Thermal denaturation procedures for hemoglobin. *Methods Enzymol.* **1994**, *231*, 514−524.
(48) Provencher, S. W.; Glockner, J. Estimation of globular protein secondary structure from circular dichroism. *Biochemistry* **1981**, *20*, 33−37.
(49) Whitmore, L.; Wallace, B. A. Protein secondary structure analyses from circular dichroism spectroscopy: Methods and reference databases. *Biopolymers* **2008**, *89*, 392−400.
(50) Sreerama, N.; Venyaminov, S. Y.; Woody, R. W. Estimation of protein secondary structure from circular dichroism spectra: Inclusion of denatured proteins with native proteins in the analysis. *Anal. Biochem.* **2000**, *287*, 243−251.
(51) Berman, H. M.; Westbrook, J.; Feng, Z.; et al. The protein data bank. *Nucleic Acids Res.* **2000**, *28*, 235−242.
(52) Arnold, K.; Bordoli, L.; Kopp, J.; Schwede, T. The SWISS-MODEL workspace: A web-based environment for protein structure homology modelling. *Bioinformatics* **2006**, *22*, 195−201.
(53) Lambright, D. G.; Noel, J. P.; Hamm, H. E.; Sigler, P. B. Structural determinants for activation of the α-subunit of a heterotrimeric G protein. *Nature* **1994**, *369*, 621−628.
(54) Sondek, J.; Lambright, D. G.; Noel, J. P.; Hamm, H. E.; Sigler, P. B. GTPase mechanism of G proteins from the 1.7-Å crystal structure of transducin α-GDP AlF_4^-. *Nature* **1994**, *372*, 276−279.
(55) Noel, J. P.; Hamm, H. E.; Sigler, P. B. The 2.2 Å crystal structure of transducin-α complexed with GTPγS. *Nature* **1993**, *366*, 654−663.
(56) Humphrey, W.; Dalke, A.; Schulten, K. VMD: Visual molecular dynamics. *J. Mol. Graph.* **1996**, *14*, 33−38.
(57) Phillips, J. C.; Braun, R.; Wang, W.; et al. Scalable molecular dynamics with NAMD. *J. Comput. Chem.* **2005**, *26*, 1781−1802.

DOI: 10.1021/acsomega.8b01174
ACS Omega 2018, 3, 12320−12329